12-1-2018

Vitamin e Promotes the Inverse Hexagonal Phase via a Novel Mechanism Implications for Antioxidant Role

Paul Harper
Calvin University

LANGMUIR

pubs.acs.org/Langmuir Article

Vitamin E Promotes the Inverse Hexagonal Phase via a Novel Mechanism: Implications for Antioxidant Role

Paul E. Harper,* Andres T. Cavazos, Jacob J. Kinnun, Horia I. Petrache, and Stephen R. Wassall

Cite This: *Langmuir* 2020, 36, 4908−4916 Read Online

ABSTRACT: Vitamin E (α-tocopherol) and a range of other biological compounds have long been known to promote the H_{II} (inverted hexagonal) phase in lipids. Now, it has been well established that purely hydrophobic lipids such as dodecane promote the H_{II} phase by relieving extensive packing stress. They do so by residing deep within the hydrocarbon core. However, we argue from X-ray diffraction data obtained with 1-palmitoyl-2-oleoylphosphatidylcholine (POPE) and 1,2-dioleoylphosphatidylcholine (DOPE) that α-tocopherol promotes the H_{II} phase by a different mechanism. The OH group on the chromanol moiety of α-tocopherol anchors it near the aqueous interface. This restriction combined with the relatively short length of α-tocopherol (as compared to DOPE and POPE) means that α-tocopherol promotes the H_{II} phase by relieving compressive packing stress. This observation offers new insight into the nature of packing stress and lipid biophysics. With the deeper understanding of packing stress offered by our results, we also explore the role that molecular structure plays in the primary function of vitamin E, which is to prevent the oxidation of polyunsaturated membrane lipids.

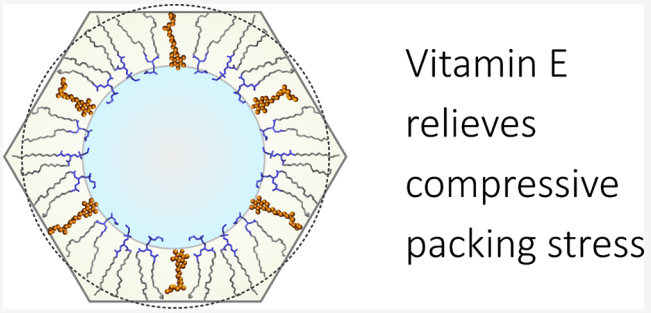

INTRODUCTION

The H_{II} or inverted hexagonal phase (see Figure 1) in lipids has long been appreciated as a window offering insight into both the biophysical properties of lipids and their interactions with proteins and other biomolecules.[1] The degree to which lipids curl, or their spontaneous curvature,[2] is revealed in the H_{II} phase and has been shown to exert a powerful effect on the conductance of the ion channel alamethicin.[3] Lung surfactant protein promotes curvature in the H_{II} phase, and this is thought to be connected to its essential role for proper pulmonary function.[4] It is known that the wasp venom mastoparan promotes the H_{II} phase and that, interestingly, inhibitors of the venom do the reverse.[5] These are just a few examples of a whole host of membrane disruptive compounds, including antimicrobial peptides, that actively promote or inhibit the H_{II} phase.[6,7]

α-Tocopherol is the form of vitamin E retained by the human body. It is a lipid-soluble antioxidant that is an essential micronutrient.[8] Symptoms of deficiency include nerve and muscle damage.[9,10] The primary role of α-tocopherol is to protect polyunsaturated phospholipids from oxidation in membranes,[11] although modulation of membrane architecture is another mode of action that has recently been examined.[12] Its molecular structure consists of a chromanol group with a hydroxyl group on the benzene ring at one end and a phytanyl chain attached at the other end (see Figure 2). In phospholipid bilayers, the hydroxyl group usually sits near the aqueous interface, while the phytanyl chain extends toward the middle of the bilayer.[13−16] The effect of α-tocopherol on the phospholipid is, somewhat akin to cholesterol, to disrupt chain packing in the gel state and to increase order in the liquid crystalline state.[17,18] Vitamin E is known to promote the H_{II} phase.[19−21] Here we present data on phosphatidylethanolamine (PE) lipids that we propose reveal that α-tocopherol induces the H_{II} phase by a new mechanism.

In terms of understanding the energetics of the H_{II} phase, there are two key components, the curvature energy and the packing energy. Following Gruner et al.[2] and more recent studies,[22−26] curvature energy represents an elastic free energy term that depends on bending rigidity and intrinsic curvature, while packing energy refers to hydrocarbon-packing free energy. The curvature energy is strongly influenced by the overall shape of the lipid and for lipids with high intrinsic curvature generally promotes curved phases such as H_{II}. On the other hand, the anisotropy of lipid lengths in the H_{II} phase gives rise to unfavorable packing energy (see Figure 1). This

Received: January 21, 2020
Revised: March 31, 2020
Published: April 15, 2020

https://dx.doi.org/10.1021/acs.langmuir.0c00176
Langmuir 2020, 36, 4908−4916

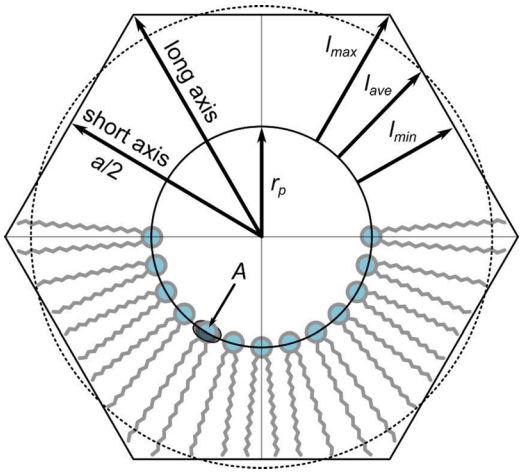

Figure 1. Diagram of a unit cell of the H_{II} phase, which consists of a lipid monolayer wrapped around a cylindrical water core. Lipids are explicitly shown in the bottom half of the diagram, with the hydrophilic heads drawn as circles and the hydrophobic tails as zigzag lines. Going from the center, one can get to the edge of the cell via the short path (which is one-half of the lattice parameter a) or via the long path. Lipid lengths are at a maximum, l_{max}, along the long path and at a minimum, l_{min}, along the short path, with the average length, l_{ave}, lying in between. A circle with a radius equal to $r_p + l_{ave}$ is drawn with a dashed line. The radius of the water core is r_p, and the average cross-sectional area per lipid at the Luzzati interface is A.

foundational model was established by a classic series of experiments that showed a purely hydrophobic compound, such as dodecane, could relieve the packing stress by filling in the interstitial corners of the H_{II} phase.[2] With the packing stress relieved, the curvature energy dominates and the lipid can express its spontaneous curvature.[27] This basic model has been used and extended with a great deal of success,[28,29] but open questions remain[30] and experimental measurements of curvature interactions remain an active area.[24,31]

We explore in this work the contrasting changes α-tocopherol and dodecane make to the H_{II} structure in POPE and DOPE and argue that these differences are due to the quite different interactions each compound has on lipids in general and the packing energy stress in particular.

MATERIALS AND METHODS

Sample Preparation. POPE (16:0−18:1 PE or 1-palmitoyl-2-oleoyl-*sn*-glycero-3-phosphoethanolamine) and DOPE (18:1−18:1 PE or 1,2-dioleoyl-*sn*-glycero-3-phosphoethanolamine) were obtained from Avanti Polar Lipids (Alabaster, AL), while α-tocopherol was prepared as previously described[15] and Sigma (St. Louis, MO) was the source for dodecane. Phospholipid (POPE or DOPE) was codissolved in chloroform with dodecane or α-tocopherol in a 2:1 or 4:1 molar ratio, respectively. The organic solvent was removed under a stream of nitrogen gas followed by vacuum pumping overnight. The dried lipid was thoroughly mixed with water and was then transferred to an Eppendorf tube, with the final composition being 3 wt % lipid (approximately 15 mg) in water. Samples containing α-tocopherol were frozen and thawed three times to abet uniform dispersion before X-ray measurements were recorded. Samples containing dodecane were not frozen and thawed as we found this procedure actually resulted in the dodecane separating out, possibly due to dodecane's lower density. We note that freezing dodecane−lipid mixtures was not part of the mixing procedure in a previous X-ray study.[32] Equivalent molar, weight, and volume compositions are listed in Table 1.

X-ray Diffraction Measurements. X-ray diffraction data were taken using a fixed-anode Bruker Nanostar U system (Bruker AXS, Madison, WI), with a typical exposure being 14 400 s (4 h) in duration. The integrated sum of three such exposures for POPE and α-tocopherol at 40 °C is shown in Figure 3. The peaks were integrated using the software package FIT2D and were Lorentz and

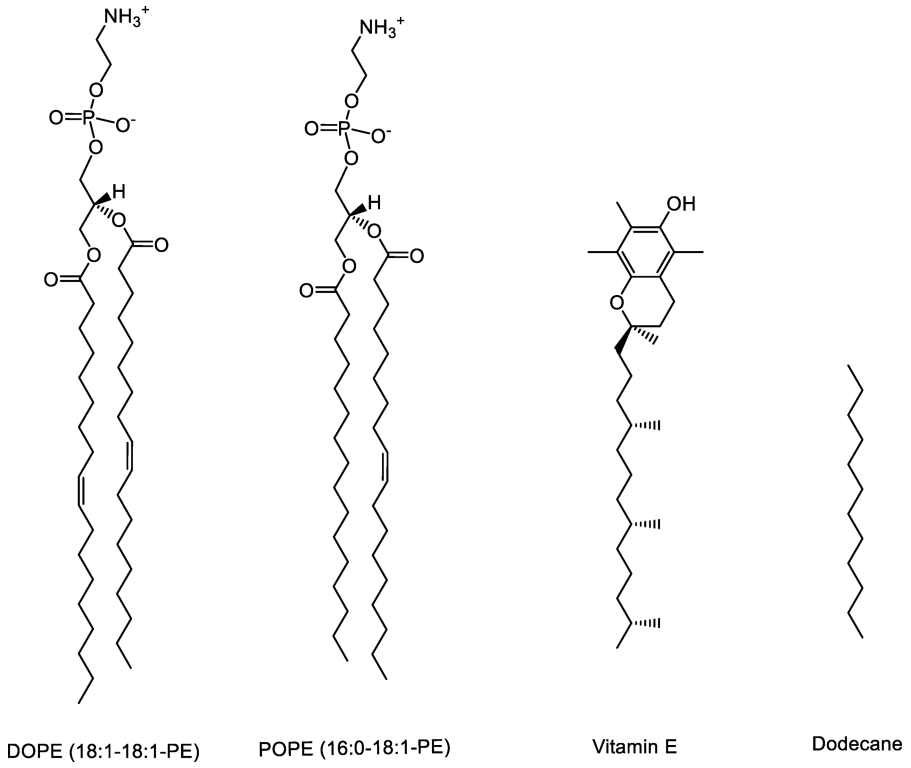

Figure 2. Chemical structures of DOPE, POPE, α-tocopherol, and dodecane.

https://dx.doi.org/10.1021/acs.langmuir.0c00176
Langmuir 2020, 36, 4908−4916

Table 1. Equivalent Molar, Weight, and Volume Compositions[a]

		equivalent compositions		
lipid	additive	mole fraction	weight fraction	volume fraction
DOPE	α-tocopherol	0.20	0.13	0.13
POPE	α-tocopherol	0.20	0.13	0.14
DOPE	dodecane	0.33	0.10	0.13
POPE	dodecane	0.33	0.11	0.14

[a]Molecular weight and density, respectively, are 744 g and 1.00 g/cm^3 (DOPE) and 718 g and 1.00 g/cm^3 (POPE), each at 50 °C.[33,34,36] The molecular weight and density, respectively, are 431 g and 0.9 ± 0.1 g/cm^3 (α-tocopherol) and 170 g and 0.8 ± 0.1 g/cm^3 (dodecane).[44] Note that the equivalent compositions for DOPE and POPE are practically identical.

multiplicity corrected.[33] The peak amplitudes thereby extracted from the data are given in Table 2.

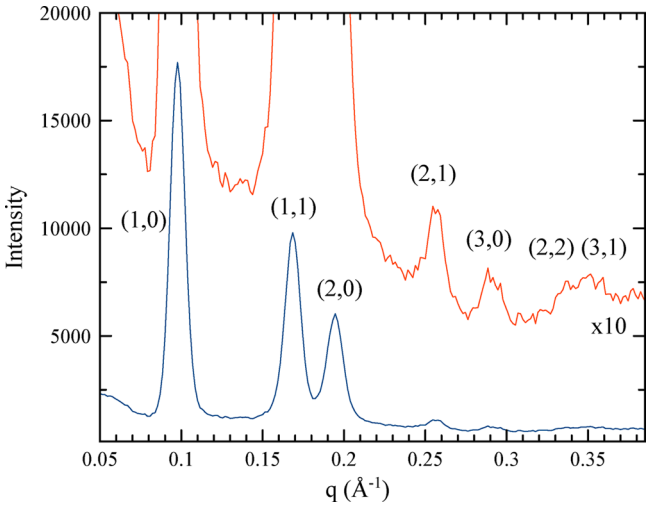

Figure 3. Integrated X-ray scattering intensity of POPE and α-tocopherol at 40 °C. The scattering pattern is typical for the H_{II} phase, and each peak is labeled by its Miller indices. The intensity ×10 is also plotted to better reveal the weaker, higher order peaks.

RESULTS

The H_{II} phase is depicted in Figure 1 and consists of a hexagonal unit cell in which a layer of lipids wraps around a cylindrical water core. The distance from the center of the cell to the edge is at a minimum along the short direction and at a maximum along the long direction. The lattice spacing, a, is the distance between the centers of adjacent water cores or, equivalently, twice the distance from the center of the cell to the edge along the short direction. The radius of the water core is r_p; it has been shown that it is located at the electron density maximum.[32,34] The thickness of the lipid layer varies from l_{min} to l_{max}, each of these being respectively measured along the short and long directions of the unit cell. The average lipid length, l_{ave}, is calculated using an area weighted average.[33] Consequently, the average lipid length assumes a value that yields roughly equal areas of compression and expansion (see Figure 1).

X-rays scatter primarily off electrons, and so diffraction data can be used to reconstruct the electron density of the lipid structures. Note that this method only gives relative electron density, $\Delta\rho$, where $\rho_{electron} = \rho_{average} + \Delta\rho$. The relative electron density can be reconstructed from the measured X-ray diffraction amplitudes and their phasings via

$$\Delta\rho = \sum_{(h,k)\neq(0,0)}^{h,k\ max} \alpha_{hk} F_{hk} \cos(\mathbf{b}_{hk}\cdot\mathbf{r}) \quad (1)$$

where h and k are the Miller indices and $\mathbf{r}$ is position. The α_{hk}, F_{hk}, and $\mathbf{b}_{hk}$ terms are, respectively, the phase, amplitude, and reciprocal lattice vector for each pair of Miller indices. Electron density reconstructions were performed and the proper phasing was determined by selecting the most physically plausible combination, that is, one that resulted in a uniform electron density peak ring corresponding to the phospholipid heads, an electron density valley in the center for the water region, and a deeper valley for the low electron density region of the hydrocarbon tails. For basic, detailed information on performing reconstructions, the reader is referred to Harper et al.[33] For recent, innovative work on reconstructions, one can also consult Frewein et al.[35] The resulting phasings were in agreement with the rubric developed in Turner and Gruner,[32] which states that for $r_p/a > 0.258$, the correct phasing is +, −, −, +, +, +, +, and for $0.237 < r_p/a < 0.258$, the correct phasing is +, −, −, −, +, +, +. These phasing combinations are also in agreement with subsequent reconstructions of lipids in the H_{II} phase.[33,36,37]

A 3-D plot of the relative electron density ($\Delta\rho$) of POPE and α-tocopherol at 40 °C is shown in Figure 4 (left panel).

Table 2. Lorentz and Multiplicity Corrected Amplitudes Calculated from Measured Peak Intensities in X-ray Data[a]

		amplitudes									
	temp (°C)	(1,0)	(1,1)	(2,0)	(2,1)	(3,0)	(2,2)	(3,1)	(4,0)	(3,2)	(4,1)
POPE and α-tocopherol	40	1.00	1.00	0.83	0.18	0.21	0.14	0.15			
	50	1.00	0.95	0.81	0.16	0.22	0.20	0.13			
POPE and dodecane	40	1.00	0.84	0.71	0.00	0.31	0.23	0.17			
	50	1.00	0.81	0.69	0.04	0.17	0.20	0.14			
DOPE and α-tocopherol	40	1.00	0.68	0.66	0.00	0.00	0.09	0.06			
	50	1.00	0.64	0.62	0.00	0.00	0.11	0.08			
DOPE and dodecane[b]	40	0.97	0.64	0.58	0.02	0.09	0.18	0.15	0.05		
	50	0.97	0.61	0.56	0.02	0.07	0.17	0.15	0.05		
DOPE[b]	40	0.95	0.87	0.73	0.13	0.18	0.17	0.14	0.02	0.03	0.04
	50	0.97	0.84	0.71	0.09	0.16	0.17	0.14	0.03	0.02	0.02

[a]Amplitudes for our data have been normalized to the first-order peak. [b]Data from Turner and Gruner.[32] The phasing for these peaks is +, −, −, +, +, +, +, +, −, −. Uncertainties in the amplitudes are of order ±0.03 relative to the first peak.

https://dx.doi.org/10.1021/acs.langmuir.0c00176
Langmuir 2020, 36, 4908−4916

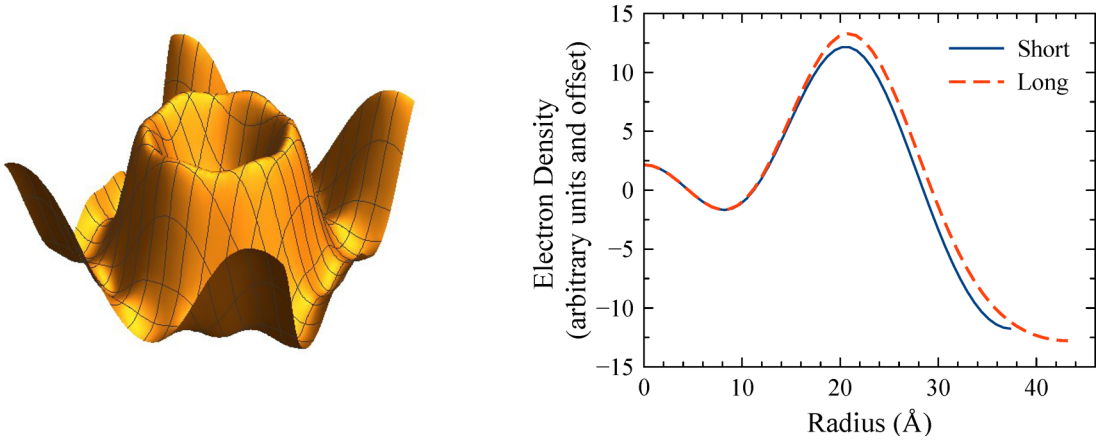

Figure 4. Relative electron density of POPE and α-tocopherol at 40 °C. Left: 3-D plot of the electron density (vertical axis) of the H_{II} phase. The high electron density phospholipid headgroups generate a ring peak with a shallow inner central valley for the aqueous region and a deeper outer valley for the hydrocarbon region. Right: Slices of the electron density along the short and long directions (see Figure 1). Note that the relative electron density maximum along the long direction ($\Delta\rho_{long}$) is slightly higher than the electron density maximum along the short direction ($\Delta\rho_{short}$).

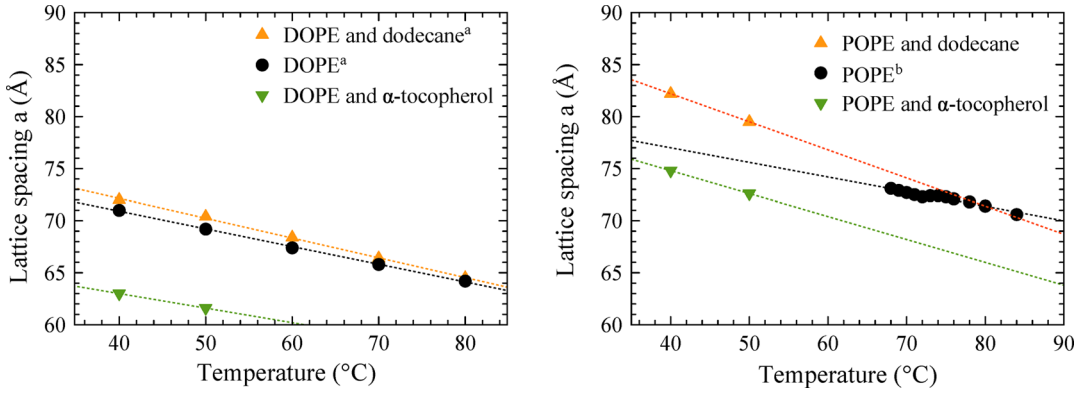

Figure 5. Lattice spacings (center of water core to center of water core distance) for DOPE (left) and POPE (right) for the lipid only, lipid with α-tocopherol, and lipid with dodecane. Linear fits of the data are displayed as dotted lines to guide the eye. For both DOPE and POPE, α-tocopherol reduces the lattice spacing, while dodecane increases it. (a) Data from Turner and Gruner.[32] (b) Data from Rappolt et al.[36]

The phospholipid headgroups form a fairly uniform peaked ring that steeply drops off in the hydrocarbon region. Slices of the electron density through the short and long directions (see Figure 1) are also shown in Figure 4 (right panel). Note that there is a good deal of rotational symmetry, which is typical for these systems. Nonetheless, there is a noticeable difference in the relative electron density along the short and long directions. The peak relative electron densities along each direction are designated as $\Delta\rho_{short}$ and $\Delta\rho_{long}$.

Figure 5 illustrates the contrasting effect that dodecane and α-tocopherol have on the structural parameters derived from our data that characterize the H_{II} phase (see Table 3). It can be seen that dodecane slightly increases the lattice parameter, a, for DOPE, whereas α-tocopherol substantially reduces it (Figure 5, left panel). A similar trend is apparent with POPE (Figure 5, right panel). As alluded to earlier, the radius r_p of the water core is the average of the radii measured for the electron density maxima along the short and long directions. Both dodecane and α-tocopherol reduce the value of r_p in DOPE (Figure 6, left panel) and POPE (Figure 6, right panel). The reduction is greater with α-tocopherol than with dodecane.

Geometry (see Figure 1) readily suffices to determine the minimum length of the lipid monolayer, l_{min}, which is

Table 3. Dimensional Parameters for the Lipid and Additive Combinations Measured in This Study[a]

	structural parameters					
	temp (°C)	a (Å)	r_p (Å)	V_{lipid} (Å^3)	l_{ave} (Å)	A (Å^2)
POPE and α-tocopherol	40	74.8	20.6	1185	18.8	50.2
	50	72.6	20.0	1190	18.3	52.0
POPE and dodecane	40	82.2	22.2	1185	21.1	44.1
	50	79.5	21.1	1190	20.8	44.5
DOPE and α-tocopherol	40	63.0	15.5	1230	17.7	51.4
	50	61.6	15.2	1238	17.3	53.0

[a]See Figure 1 for the geometric definitions of the parameters and the Results for how the parameters were calculated. Note that the average lipid length, l_{ave}, includes both the lipid and the additive (if present). Uncertainties for the linear quantities (a, r_p, l_{ave}) are ±0.5 Å, with the uncertainty for the volume being ±20 Å^3 and for the area being ±2 Å^2.

$$l_{min} = a/2 - r_p \quad (2)$$

and the maximum length of the lipid monolayer, l_{max}, which is

$$l_{max} = \frac{a/2}{\cos \pi/6} - r_p \quad (3)$$

https://dx.doi.org/10.1021/acs.langmuir.0c00176
Langmuir 2020, 36, 4908−4916

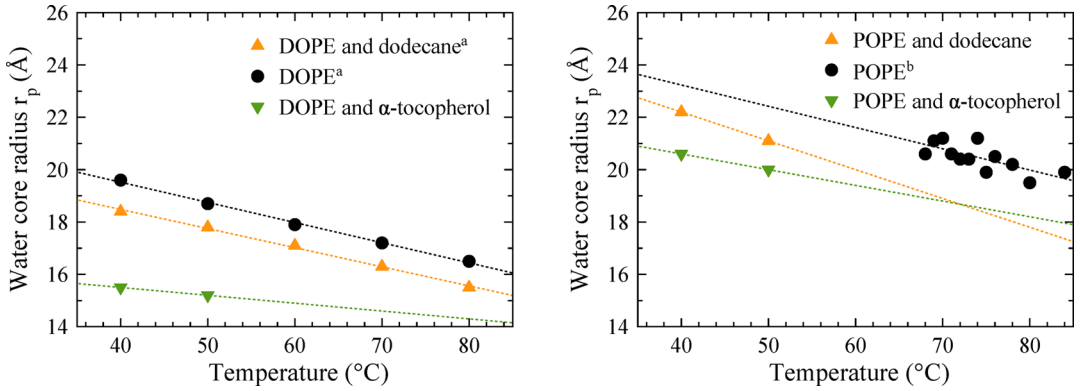

Figure 6. Water core radii for DOPE (left) and POPE (right) for the lipid only, lipid with α-tocopherol, and lipid with dodecane. Linear fits of the data are displayed as dotted lines to guide the eye. For both DOPE and POPE, the water core radius is reduced by α-tocopherol and, to a lesser amount, dodecane. (a) Data from Turner and Gruner.[32] (b) Data from Rappolt et al.[36]

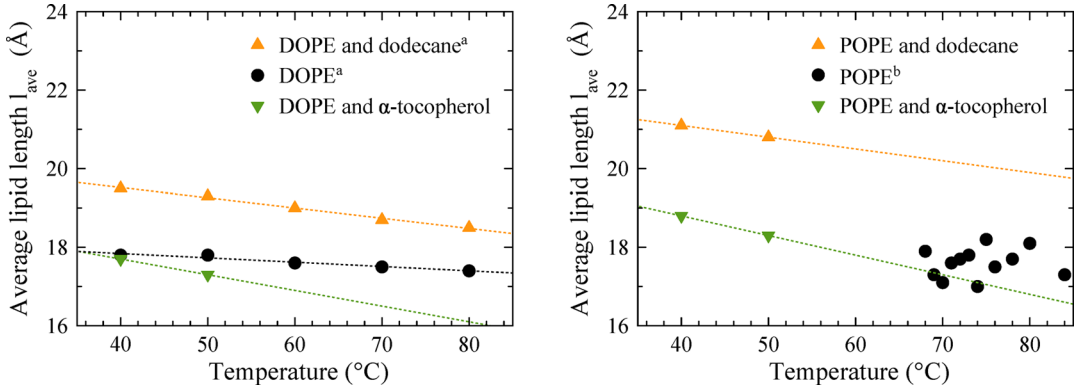

Figure 7. Average lipid lengths for DOPE (left) and POPE (right) for the lipid only, lipid with α-tocopherol, and lipid with dodecane. Linear fits of the data are displayed as dotted lines to guide the eye. For both DOPE and POPE, α-tocopherol does not substantially change the average length, but dodecane increases it. (a) Data from Turner and Gruner.[32] (b) Data from Rappolt et al.[36]

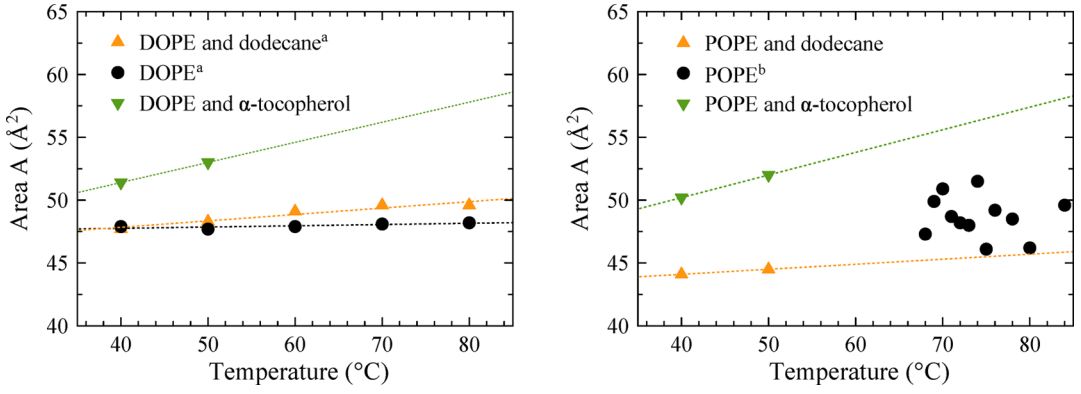

Figure 8. Average areas for DOPE (left) and POPE (right) for the lipid only, lipid with α-tocopherol, and lipid with dodecane. Linear fits of the data are displayed as dotted lines to guide the eye. In general, α-tocopherol increases the area, while dodecane does not seem to greatly change it. (a) Data from Turner and Gruner.[32] (b) Data from Rappolt et al.[36]

The average lipid length can be calculated by taking an area weighted average of the length of the lipid monolayer. Note that in this Article lipid includes both the membrane forming lipid (DOPE or POPE) and the additive (dodecane or α-tocopherol). It can be shown[33] that the average lipid length is well approximated by

$$l_{ave} = (a/2 - r_p)\left[1.1084 + 0.0572\left(\frac{r_p}{a/2 - r_p} - 1\right)\right] \quad (4)$$

We accordingly see that dodecane increases the average lipid length, as opposed to α-tocopherol that leaves it generally unchanged (see Figure 7).

The cross-section area per lipid A at the lipid–water interface (Figure 1) can be found by

$$A = V_{total}\left(\frac{2\pi r_p}{\sqrt{3}\,a^2/2 - \pi r_p^2}\right) \quad (5)$$

https://dx.doi.org/10.1021/acs.langmuir.0c00176
Langmuir 2020, 36, 4908−4916

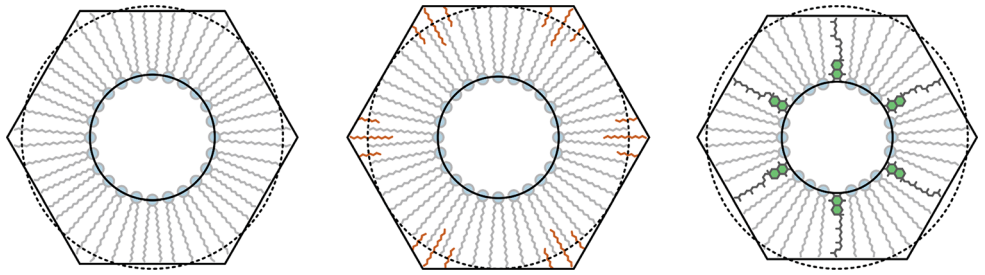

Figure 9. Models for PE-only, PE and dodecane, and PE and α-tocopherol in the H_{II} phase. Dodecane fits in deep in the hydrocarbon tail region, predominantly along the long direction. By contrast, α-tocopherol fills in along the short direction and is relatively close to the lipid−water interface. For all of the diagrams, the dashed circle indicates the average lipid length found in the PE-only case. As discussed in the text, dodecane enlarges the unit cell so that the average lipid length in the PE-only case matches the minimum lipid length in the PE and dodecane case. Likewise, α-tocopherol reduces the unit cell size, and the average lipid length for the PE-only case is closer to the maximum lipid length in the PE and α-tocopherol case.

Table 4. In Depth Comparative Listing of DOPE H_{II} Dimensions for DOPE-Only and with Either Dodecane or α-Tocopherol at a Single Temperature (40 °C)[a]

	detailed DOPE dimensions at 40 °C							
	a (Å)	r_p (Å)	$\Delta\rho_{long}/\Delta\rho_{short}$	l_{ave} (Å)	l_{min} (Å)	l_{max} (Å)	$l_{max} - l_{min}$ (Å)	A (Å^2)
DOPE-only[b]	71.0	19.6	1.09	17.8	15.9	21.4	5.5	47.9
DOPE and dodecane[b]	72.0	18.4	1.09	19.5	17.6	23.2	5.6	47.7
DOPE and α-tocopherol	63.0	15.5	1.15	17.7	16.0	20.8	4.9	51.4

[a]Note that the lipid lengths include both the lipid and the additive (if present). [b]Data from Turner and Gruner.[32] Uncertainties are as in Table 3, with the uncertainty in $\Delta\rho_{long}/\Delta\rho_{short}$ being ±0.06.

where, as before, a is the lattice size, r_p is the water core radius, and $V_{total} = V_{lipid} + V_{additive}$.[33] Note that this definition of the area per lipid follows a volumetric decomposition of the unit cell as introduced by Luzzati et al.[1] and as shown in Figure 1. Because the volume fraction for both additives is about 0.13 (see Table 1), we note that therefore $V_{total} = V_{lipid} + 0.13V_{total}$ and hence $V_{total} = V_{lipid}/0.87$. It is apparent that the area stays roughly the same with the addition of dodecane but, in contrast, increases with α-tocopherol (see Figure 8).

DISCUSSION

It has long been appreciated that the extension of lipids in the long direction in the H_{II} phase is energetically costly, with this cost being known as the packing energy.[2] What is less appreciated is that an essential consequence of this energetically costly extension in the long direction must be necessarily accompanied by a similarly costly compression in the short direction (see Figure 1). This is readily understood by the following argument. Overextension in the long direction can be relieved by shrinking the thickness of the lipid monolayer in the H_{II} unit cell. One would then expect that shrinking to continue until opposed by the energetic cost of compression along the short direction. A similar argument can be made by modeling the free energy of the lipid as a harmonic function of lipid length with the minimum sensibly located at the average lipid length. Both lipid lengths longer and shorter than the average then would necessarily result in free energy costs.

α-Tocopherol and Dodecane Stabilize the H_{II} Phase by Different Mechanisms. With this model in mind, we can consider how dodecane relieves packing strain and promotes the H_{II} phase. The wholly hydrophobic structure of dodecane ensures that it will be located in the tail region of the H_{II} phase as schematically depicted in Figure 9 (middle panel). This location has been confirmed by neutron scattering experiments.[38] Consequently, it is not surprising that the interfacial area per lipid remains basically unchanged (see Table 4). Classic packing energy theory informs us that it alleviates stress in the long direction, thereby promoting the H_{II} phase.[2] Hence, the dodecane should primarily be located in this region (see Figure 9). At this point, our deeper appreciation of the dual stresses of extension and compression can now lead us into a fuller understanding of the host lipid and dodecane structure. By effectively extending the lipid lengths (see Figure 9, middle panel), the dodecane not only relieves the extension stress, but consequently also relaxes the compression stress, allowing the lipid along the short direction to relax to its optimum value. This can be seen quantitatively in that the l_{min} for DOPE and dodecane matches the l_{ave} for DOPE-only (see Table 4).

Turning to α-tocopherol, we see a rather different situation. Instead of increasing l_{max} as dodecane does, l_{max} is reduced by α-tocopherol (see Table 4). For this reason alone, it seems highly unlikely that α-tocopherol works as a lipid length extender as dodecane does. Furthermore, although mostly nonpolar, α-tocopherol does have a polar OH group at its tip. This group would tend to locate in the vicinity of the aqueous interface,[14−16,39] suggesting α-tocopherol would not find an energetic minimum deep in the nonpolar region as dodecane does. Support for this position is seen in the interfacial area per lipid, which goes up upon the addition of α-tocopherol (see Figure 8). Therefore, we propose that α-tocopherol relieves stress and promotes the H_{II} phase by replacing lipids along the short direction (see Figure 9, right panel). As noted earlier, the extensive and compressive stresses are interlocked; one drives the other, so that if one of the stresses is relieved, the other is also reduced. Hence, by alleviating the compressive stress, α-tocopherol allows a reduction in the extensive stress, resulting in a reduced l_{max}, which is what we observe (see Table 4).

In addition to our central argument, there is a suggestive pattern in how the electron density headgroup maximum

https://dx.doi.org/10.1021/acs.langmuir.0c00176
Langmuir 2020, 36, 4908−4916

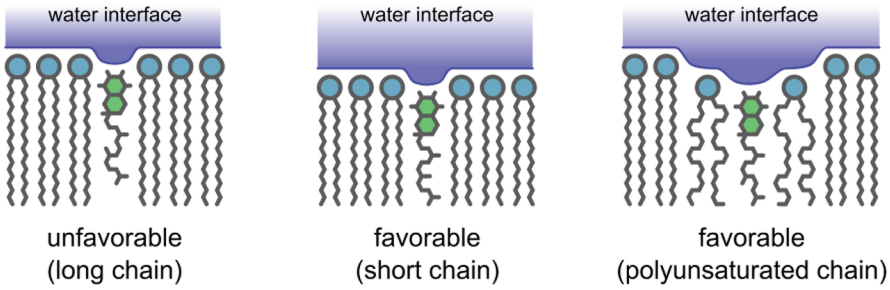

Figure 10. Model for the location of α-tocopherol in a membrane. A single monolayer is shown. The location is unfavorable when there is a mismatch between chain length (left panel) and favorable when chain lengths match (middle panel). In a mixed membrane, α-tocopherol locates next to polyunsaturated phospholipids to match chain length (right panel).

varies. We have calculated $\Delta\rho_{long}/\Delta\rho_{short}$, the ratio of the electron density maximum along the long direction relative to the short direction. The electron density maximum is due to the electron dense phosphorus headgroups; with α-tocopherol as the additive, these headgroups are displaced in the short direction, presumably resulting in a reduced electron density maximum. This would result in an increase in $\Delta\rho_{long}/\Delta\rho_{short}$, which is what we see for our data in Table 4. However, the magnitude of the difference of this ratio between samples with and without α-tocopherol is approximately equal to its uncertainty, making this only a suggestive observation in support of our model.

We do not mean to imply, however, that this mechanism is exclusive to α-tocopherol. Other lipophilic molecules that anchor a headgroup at the aqueous interface, such as cholesterol, also induce the formation of the H_{II} phase.[22] In fact, the contrasting effects of α-tocopherol and dodecane might generalize to other similar chemical compounds.

Biological Implications. Vitamin E is a lipophilic antioxidant.[11] To protect lipids from oxidative attack is the primary function of this essential constituent in membranes and is also the basis for its use as a preservative in food and cosmetics. The chemistry involved, whereby the OH group on the chromanol group is sacrificed to terminate the chain of reactions by which the lipid peroxidation progresses, is well understood.[40] Whether there is a structural component that encourages proximity to polyunsaturated phospholipids, the lipid species most vulnerable to oxidation, remains an unanswered question.[18] The behavior of PE when vitamin E is introduced offers potential insight.

Promotion of negative curvature is revealed by the reduction in the temperature of the lamellar to H_{II} phase transition for POPE when α-tocopherol is added. It has been suggested that membranes with intrinsic, negative curvature are less permeable to oxygen.[41] The impact of vitamin E on the local architecture of membranes around PE, thus, may contribute to prevention of oxidation. Interestingly, moreover, polyunsaturated fatty acids (PUFA) are often preferentially taken up into PE.[42] From the results presented here, we also can affirm that matching lipid lengths, avoiding hydrophobic mismatch, is a profound driving force behind lipid organization. It makes sense that in a lipid bilayer, as illustrated in Figure 10, α-tocopherol will seek to be next to lipids of a similar length. As the length of the chain (12 carbons) in α-tocopherol's tail is less than that of the chain in a typical membrane phospholipid (16−18 carbons), this means that α-tocopherol will generally find its best match with membrane lipids that have effectively shorter chains (Figure 9, middle panel). The projected length of PUFA chains is shorter because their multiple double bonds confer tremendous disorder[43] so, we suggest, α-tocopherol will naturally gravitate toward polyunsaturated lipids (Figure 10).

CONCLUSIONS

In summary, we present evidence from electron density reconstructions that α-tocopherol promotes the H_{II} phase in PE by a new means, by relieving compressive stress. This mechanism contrasts with the well-studied means by which dodecane promotes the H_{II} phase, which is by reducing extensive stress. Our findings give us new insight both into the nature of packing stress and into the interactions of molecules within the lipid membrane, offering potential insight into the biological function of α-tocopherol.

AUTHOR INFORMATION

Corresponding Author

Paul E. Harper − *Department of Physics and Astronomy, Calvin University, Grand Rapids, Michigan 49546-4403, United States;* orcid.org/0000-0002-5235-9715; Phone: (616) 526-6408; Email: pharper@calvin.edu; Fax: (616) 526-6501

Authors

Andres T. Cavazos − *Department of Physics, IUPUI, Indianapolis, Indiana 46202-3273, United States*

Jacob J. Kinnun − *Department of Physics, IUPUI, Indianapolis, Indiana 46202-3273, United States*

Horia I. Petrache − *Department of Physics, IUPUI, Indianapolis, Indiana 46202-3273, United States*

Stephen R. Wassall − *Department of Physics, IUPUI, Indianapolis, Indiana 46202-3273, United States*

Complete contact information is available at: https://pubs.acs.org/10.1021/acs.langmuir.0c00176

Notes

The authors declare no competing financial interest.

ACKNOWLEDGMENTS

Funding for P.E.H. from Calvin University and the Calvin University Alumni Association is gratefully acknowledged. P.E.H. is also thankful to IUPUI (Indiana University, Purdue University at Indianapolis) for hosting his sabbatical. We would also like to thank Matthew L. Link for making some additional electron density calculations and Samuel W. Canner for help with figure preparation.

https://dx.doi.org/10.1021/acs.langmuir.0c00176
Langmuir 2020, 36, 4908−4916

REFERENCES

(1) Luzzati, V.; Reiss-Husson, F.; Rivas, E.; Gulik-Krzywicki, T. Structure and polymorphism in lipid-water systems, and their possible biological implications. *Ann. N. Y. Acad. Sci.* **1966**, *137*, 409−413.

(2) Gruner, S. M. Intrinsic curvature hypothesis for biomembrane lipid composition: a role for nonbilayer lipids. *Proc. Natl. Acad. Sci. U. S. A.* **1985**, *82*, 3665−3669.

(3) Keller, S. L.; Bezrukov, S. M.; Gruner, S. M.; Tate, M. W.; Vodyanoy, I.; Parsegian, V. A. Probability of alamethicin conductance states varies with nonlamellar tendency of bilayer phospholipids. *Biophys. J.* **1993**, *65*, 23−27.

(4) Chavarha, M.; Loney, R.; Rananavare, S.; Hall, S. Hydrophobic Surfactant Proteins Strongly Induce Negative Curvature. *Biophys. J.* **2015**, *109*, 95−105.

(5) Tytler, E. M.; Segrest, J. P.; Epand, R. M.; Nie, S. Q.; Epand, R. F.; Mishra, V. K.; Venkatachalapathi, Y. V.; Anantharamaiah, G. M. Reciprocal effects of apolipoprotein and lytic peptide analogs on membranes. Cross-sectional molecular shapes of amphipathic alpha helixes control membrane stability. *J. Biol. Chem.* **1993**, *268*, 22112−22118.

(6) Epand, R. M. Lipid polymorphism and protein−lipid interactions. *Biochim. Biophys. Acta, Rev. Biomembr.* **1998**, *1376*, 353−368.

(7) Hickel, A.; Danner-Pongratz, S.; Amenitsch, H.; Degovics, G.; Rappolt, M.; Lohner, K.; Pabst, G. Influence of antimicrobial peptides on the formation of nonlamellar lipid mesophases. *Biochim. Biophys. Acta, Biomembr.* **2008**, *1778*, 2325−2333.

(8) Niki, E.; Traber, M. G. A history of Vitamin E. *Ann. Nutr. Metab.* **2012**, *61*, 207−212.

(9) Traber, M. G. Vitamin E inadequacy in humans: causes and consequences. *Adv. Nutr.* **2014**, *5*, 503−514.

(10) Ulatowski, L. M.; Manor, D. Vitamin E and neurodegeneration. *Neurobiol. Dis.* **2015**, *84*, 78−83.

(11) Traber, M. G.; Atkinson, J. Vitamin E, antioxidant and nothing more. *Free Radical Biol. Med.* **2007**, *43*, 4−15.

(12) DiPasquale, M.; Nguyen, M. H. L.; Rickeard, B. W.; Cesca, N.; Tannous, C.; Castillo, S. R.; Katsaras, J.; Kelley, E. G.; Heberle, F. A.; Marquardt, D. The antioxidant vitamin E as a membrane raft modulator: Tocopherols do not abolish lipid domains. *Biochim. Biophys. Acta, Biomembr.* **2020**, 183189.

(13) Atkinson, J.; Epand, R. F.; Epand, R. M. Tocopherols and tocotrienols in membranes: A critical review. *Free Radical Biol. Med.* **2008**, *44*, 739−764.

(14) Marquardt, D.; Kucerka, N.; Katsaras, J.; Harroun, T. A. α-Tocopherol's location in membranes is not affected by their composition. *Langmuir* **2015**, *31*, 4464−4472.

(15) Leng, X.; Kinnun, J. J.; Marquardt, D.; Ghefli, M.; Kučerka, N.; Katsaras, J.; Atkinson, J.; Harroun, T. A.; Feller, S. E.; Wassall, S. R. α-Tocopherol is well designed to protect polyunsaturated phospholipids: MD simulations. *Biophys. J.* **2015**, *109*, 1608−1618.

(16) Ausili, A.; de Godos, A. M.; Torrecillas, A.; Aranda, F. J.; Corbalan-Garcia, S.; Gomez-Fernandez, J. C. The vertical location of α-tocopherol in phosphatidylcholine membranes is not altered as a function of the degree of unsaturation of the fatty acyl chains. *Phys. Chem. Chem. Phys.* **2017**, *19*, 6731−6742.

(17) Suzuki, Y. J.; Tsuchiya, M.; Wassall, S. R.; Choo, Y. M.; Govil, G.; Kagan, V. E.; Packer, L. Structural and dynamic membrane properties of alpha-tocopherol and. alpha-tocotrienol: Implication to the molecular mechanism of their antioxidant potency. *Biochemistry* **1993**, *32*, 10692−10699.

(18) Atkinson, J.; Harroun, T.; Wassall, S. R.; Stillwell, W.; Katsaras, J. The location and behavior of α-tocopherol in membranes. *Mol. Nutr. Food Res.* **2010**, *54*, 641−651.

(19) Nakajima, K.; Utsumi, H.; Kazama, M.; Hamada, A. α-Tocopherol-Induced Hexagonal H_{II} Phase Formation in Egg Yolk Phosphatidylcholine Membranes. *Chem. Pharm. Bull.* **1990**, *38*, 1−4.

(20) Bradford, A.; Atkinson, J.; Fuller, N.; Rand, R. The effect of vitamin E on the structure of membrane lipid assemblies. *J. Lipid Res.* **2003**, *44*, 1940−1945.

(21) Wang, X.; Quinn, P. J. The structure and phase behaviour of α-tocopherol-rich domains in 1-palmitoyl-2-oleoyl-phosphatidylethanolamine. *Biochimie* **2006**, *88*, 1883−1888.

(22) Kollmitzer, B.; Heftberger, P.; Rappolt, M.; Pabst, G. Monolayer spontaneous curvature of raft-forming membrane lipids. *Soft Matter* **2013**, *9*, 10877−10884.

(23) Perutkova, S.; Daniel, M.; Rappolt, M.; Pabst, G.; Dolinar, G.; Kralj-Iglic, V.; Iglic, A. Elastic deformations in hexagonal phases studied by small-angle X-ray diffraction and simulations. *Phys. Chem. Chem. Phys.* **2011**, *13*, 3100−3107.

(24) Tang, T. Y. D.; Brooks, N. J.; Ces, O.; Seddon, J. M.; Templer, R. H. Structural studies of the lamellar to bicontinuous gyroid cubic (Q(II)(G)) phase transitions under limited hydration conditions. *Soft Matter* **2015**, *11*, 1991−1997.

(25) Campelo, F.; Arnarez, C.; Marrink, S.; Kozlov, M. Helfrich model of membrane bending: From Gibbs theory of liquid interfaces to membranes as thick anisotropic elastic layers. *Adv. Colloid Interface Sci.* **2014**, *208*, 25−33.

(26) Siegel, D. Fourth-Order Curvature Energy Model for the Stability of Bicontinuous Inverted Cubic Phases in Amphiphile-Water Systems. *Langmuir* **2010**, *26*, 8673−8683.

(27) Tate, M. W.; Eikenberry, E. F.; Turner, D. C.; Shyamsunder, E.; Gruner, S. M. Nonbilayer phases of membrane lipids. *Chem. Phys. Lipids* **1991**, *57*, 147−164.

(28) Kozlov, M. M.; Leikin, S.; Rand, R. P. Bending, hydration and interstitial energies quantitatively account for the hexagonal-lamellar-hexagonal reentrant phase transition in dioleoylphosphatidylethanolamine. *Biophys. J.* **1994**, *67*, 1603−1611.

(29) Duesing, P. M.; Templer, R. H.; Seddon, J. M. Quantifying packing frustration energy in inverse lyotropic mesophases. *Langmuir* **1997**, *13*, 351−359.

(30) Shearman, G.; Ces, O.; Templer, R. Towards an understanding of phase transitions between inverse bicontinuous cubic lyotropic liquid crystalline phases. *Soft Matter* **2010**, *6*, 256−262.

(31) Reese, C. W.; Strango, Z. I.; Dell, Z. R.; Tristram-Nagle, S.; Harper, P. E. Structural insights into the cubic-hexagonal phase transition kinetics of monoolein modulated by sucrose solutions. *Phys. Chem. Chem. Phys.* **2015**, *17*, 9194−9204.

(32) Turner, D. C.; Gruner, S. M. X-ray diffraction reconstruction of the inverted hexagonal (HII) phase in lipid-water systems. *Biochemistry* **1992**, *31*, 1340−1355.

(33) Harper, P. E.; Mannock, D. A.; Lewis, R. N. A. H.; McElhaney, R. N.; Gruner, S. M. X-ray diffraction structures of some phosphatidylethanolamine lamellar and inverted hexagonal phases. *Biophys. J.* **2001**, *81*, 2693−2706.

(34) Tate, M. W.; Gruner, S. M. Temperature dependence of the structural dimensions of the inverted hexagonal (HII) phase of phosphatidylethanolamine-containing membranes. *Biochemistry* **1989**, *28*, 4245−4253.

(35) Frewein, M. P. K.; Rumetshofer, M.; Pabst, G. Global small-angle scattering data analysis of inverted hexagonal phases. *J. Appl. Crystallogr.* **2019**, *52*, 403−414.

(36) Rappolt, M.; Hickel, A.; Bringezu, F.; Lohner, K. Mechanism of the Lamellar/Inverse Hexagonal Phase Transition Examined by High Resolution X-Ray Diffraction. *Biophys. J.* **2003**, *84*, 3111−3122.

(37) Rappolt, M.; Hodzic, A.; Sartori, B.; Ollivon, M.; Laggner, P. Conformational and hydrational properties during the $L_{\beta'}$- to L_{α}- and L_{α}- to H_{II}-phase transition in phosphatidylethanolamine. *Chem. Phys. Lipids* **2008**, *154*, 46−55.

(38) Turner, D. C.; Gruner, S. M.; Huang, J. S. Distribution of decane within the unit-cell of the inverted hexagonal (HII) phase of lipid water decane systems determined by neutron-diffraction. *Biochemistry* **1992**, *31*, 1356−1363.

(39) Qin, S.-S.; Yu, Z.-W.; Yu, Y.-X. Structural and Kinetic Properties of α-Tocopherol in Phospholipid Bilayers, a Molecular Dynamics Simulation Study. *J. Phys. Chem. B* **2009**, *113*, 16537−16546.

https://dx.doi.org/10.1021/acs.langmuir.0c00176
Langmuir 2020, 36, 4908−4916

(40) Burton, G.; Ingold, K. U. Vitamin E: application of the principles of physical organic chemistry to the exploration of its structure and function. *Acc. Chem. Res.* **1986**, *19*, 194−201.
(41) Li, Q.-T.; Yeo, M. H.; Tan, B. K. Lipid peroxidation in small and large phospholipid unilamellar vesicles induced by water-soluble free radical sources. *Biochem. Biophys. Res. Commun.* **2000**, *273*, 72−76.
(42) Wassall, S. R.; Stillwell, W. Polyunsaturated fatty acid-cholesterol interactions: domain formation in membranes. *Biochim. Biophys. Acta, Biomembr.* **2009**, *1788*, 24−32.
(43) Stillwell, W.; Wassall, S. R. Docosahexaenoic acid: membrane properties of a unique fatty acid. *Chem. Phys. Lipids* **2003**, *126*, 1−27.
(44) ChemScr, CAS Number Index. http://wwww.chemsrc.com/en/casindex/, 2018.

https://dx.doi.org/10.1021/acs.langmuir.0c00176
Langmuir 2020, 36, 4908−4916